Biotoxic trace metal ion detection by enzymatic inhibition of a glucose biosensor based on a poly(brilliant green)–deep eutectic solvent/carbon nanotube modified electrode

Wanderson da Silva, Mariana Emilia Ghica, ChristopherM.A. Brett *

Department of Chemistry, Faculty of Sciences and Technology, University of Coimbra, 3004-535, Coimbra, Portugal

ARTICLE INFO

ABSTRACT

A highly sensitive glucose oxidase (GOx) electrochemical biosensor for the determination of the biotoxic trace metal ions Hg^{2+}, Cd^{2+}, Pb^{2+} and Cr^{VI} by enzyme inhibition has been developed. GOx was immobilized on a novel sensing platform consisting of poly(brilliant green) films formed by potential cycling electropolymerization in sulfuric acid doped ethaline deep eutectic solvent on multiwalled carbon nanotube modified glassy carbon electrodes. Polymer films produced in this medium presented more uniform morphology and better electrochemical sensing properties than those prepared in aqueous solution. The inhibitor concentration necessary to give 50% inhibition, I_{50}, was used for the determination of the type of reversible inhibition, and the relationship between I_{50} and the inhibition constant K_i is discussed. The new biosensor was successfully used for the determination of biotoxic trace metal ions with a nanomolar limit of detection, lower than in the literature, very good repeatability, stability and selectivity, and was applied successfully to detection of the toxic trace metal species in milk samples.

1. Introduction

The toxicological or nutritional implications of metallic species are directly related with the group of metals in the periodic table to which they belong and/or the amounts absorbed by living organisms, which can lead to chronic poisoning [1,2]. Excessive bioaccumulation of toxic metal ion traces including Hg^{2+}, Cd^{2+}, Pb^{2+}, and Cr^{VI}, have been reported as being responsible for a variety of health problems such as mammalian cancer, damage to the nervous system, brain function, and of other organs such as the heart, kidney, and lungs, leading to respiratory disease or even death [3–6]. Thus, the procurement of a fast, accurate and reliable analytical approach for monitoring toxic trace metals in the environment for humans and other organisms has received considerable attention.

Enzyme-based electrochemical biosensors have emerged as an efficient alternative to traditional analytical methods for the analysis of trace metal ions, that have drawbacks such as being time-consuming, high-cost, requiring complex instrumentation and highly specialized staff, and lack of suitability for on-field analysis [7–11]. Advantages of electrochemical detection include simple sensor preparation, fast response, excellent sensitivity, and selectivity. Enzyme-inhibition biosensors, to date, offer one of the best choices for the simple and rapid de-tection of toxic compounds such as pesticides and heavy metal ions due to their selective inhibition of enzyme activity [12]. Furthermore, the achievable limit of detection is often much lower, nanomolar, than that obtained by purely electrochemical methods and it can quantify concentration values less than the specified maximum allowed values in clinical and environmental samples [13]. However, the choice of suitable platforms for enzyme immobilization is mandatory since this may influence biocompatibility, catalytic properties, stability and sensitivity, as well as retention of enzyme activity. Therefore, to fabricate a biosensor with high performance, efforts need to be made in the development of new and advanced electrode materials.

Deep eutectic solvents (DES) are formed by a binary mixture composed of a hydrogen bond donor (HBD) and acceptor (HBA) mixed in a specific molar ratio. DES exhibit similar properties to ionic liquids that include high conductivity, stability, non-toxicity, and a wider potential range than aqueous solutions, permitting the preparation of materials with controlled structure for sensor applications [14]. However, the development of conducting and redox polymer-modified electrodes using DES as electrolyte has been little explored so far. The few articles that report their use in polymer electrodeposition highlight the formation of polymer films with better performance in terms of film conductivity than their analogues synthesized in aqueous solution [15–19].

This work describes, for the first time, the development of a biosensor based on GOx immobilized on novel ultra-thin poly(brilliant green) (PBG) films electrodeposited in ethaline DES on multiwalled carbon nanotube (MWCNT) modified glassy carbon electrodes (GCE) for inhibitive amperometric detection of Hg^{2+}, Cd^{2+}, Pb^{2+}, and Cr^{VI}. The influence of different doping agents (SO_4^{2-}, NO_3^-, Cl^-, and COO^-) and of scan rate on the electrodeposition of PBG was probed. The performance of the nanocomposite modified GCE was evaluated by cyclic voltammetry (CV). Scanning electron microscopy (SEM) was used to examine the morphology of the nanostructures and its influence on electrochemical properties. Comparison with PBG films electrodeposited in aqueous solution was also made. In the fabrication of the biosensor, other factors were also considered, such as the influence of the electrode modifiers on the degree of GOx inhibition, operational stability, sensitivity, and reproducibility. The elucidation of the mechanism of reversible inhibition for each ion was done by a novel method [20].

2. Experimental

2.1. Reagents and solutions

Glucose oxidase type X–S (from *Aspergillus Niger*, activity 15,100 $U g^{-1}$, CAS number: 9001-37-0), bovine serum albumin (BSA), glutaraldehyde (GA, 2.5% v/v in water), sulfuric acid (97%), nitric acid (65%), hydrochloric acid (37%), acetic acid (94.74%), choline chloride, and anhydrous ethylene glycol were purchased from Sigma-Aldrich, Germany. Brilliant green dye (95%) was purchased from Fluka, Switzerland. MWCNT with ~95% purity, diameter 30 ± 10 nm, and $1–5 \mu m$ length were from Nanolab, U.S.A. For the study of inhibition, standard $1000 mg L^{-1}$ solutions (Tec-Lab, Brazil) of Hg^{2+} (traceable to SRM 3133 NIST, USA), Pb^{2+} (traceable to SRM 3128 NIST, USA), Cd^{2+} (traceable to SRM 3108 NIST, USA), and Cr^{VI} (potassium dichromate from Sigma-Aldrich, Germany) were used. The McIlvaine buffer solution pH 4.0, was prepared by mixing 0.1 M citric acid (Sigma-Aldrich) and 0.2 M Na_2HPO_4 (Riedel-de-Haen). The phosphate buffer (PB) supporting electrolyte solution was prepared by mixing NaH_2PO_4 (Riedel-de-Haen) and $Na_2HPO_4 \cdot 2H_2O$ (Fluka) and adjusting the pH with 0.1 mM hydrochloric acid or 0.1 mM sodium hydroxide (Sigma-Aldrich).

All reagents were of analytical grade and were used without further purification. Millipore Milli-Q nanopure water (resistivity $\geq 18 M\Omega$ cm) was used for the preparation of all solutions. Experiments were performed at room temperature ($25 \pm 1 \,°C$).

2.2. Instrumentation

Voltammetric and amperometric experiments were carried out with a computer-controlled Ivium Compactstat potentiostat (Ivium Technologies B·V Eindhoven, Netherlands). For all electrochemical experiments, a conventional three-electrode system consisting of a $0.00785 cm^2$ geometric area glassy carbon electrode (GCE) as working electrode, a platinum wire counter electrode, and an Ag/AgCl (3 M KCl) reference electrode were used.

Surface morphological images of the nanostructured materials electrodeposited on carbon film electrodes were obtained using scanning electron microscopy (SEM) with a JEOL, JSM-5310, Japan. The pH measurements were made with a CRISON 2001 micro pH-meter (Crison Instruments SA, Barcelona, Spain).

2.3. Functionalization and preparation of carbon nanotubes (MWCNT) in chitosan solution

Prior to use, MWCNT were functionalized in nitric acid as described previously [21], by dispersion and stirring in 5 M nitric acid for 24 h.

This treatment was performed in order to ensure complete removal of impurities obtained during their production, as well as of amorphous carbon. Nitric acid also causes some significant defects in carbon nanotube structures and insertion of some negative –COO^- groups, improving their conductivity [22,23]. The functionalized MWCNT were then filtered and washed with Milli-Q water until neutral and dried in an oven at 80 °C overnight. In order to modify the GCE with the functionalized MWCNT, dispersions of 1.0% w/v MWCNT was prepared in 0.2%, 0.5%, and 1.0% w/v chitosan dissolved in 1.0% v/v acetic acid and was sonicated for 2 h to ensure complete homogeneity of the mixture. Prior to modification, the bare GCE was mechanically polished with diamond spray on a polishing cloth (Kemet, UK) down to 1 µm particle size, leading to a mirror-like surface. The polished electrode was rinsed and sonicated to remove any adherent solid particles. After the cleaning procedure, 1 µL of the one of the three different MWCNT-chitosan dispersion solutions was drop cast two times on the GCE surface and left to dry at room temperature for ~ 60 min for each drop. Before polymerization procedures, the stability of the MWCNT-chitosan films was assessed by the immersion of the modified electrodes in aqueous solution containing 0.5 M H_2SO_4. MWCNT-chitosan films prepared by using the dispersions containing 0.2% and 0.5% chitosan loading, detached immediately from the electrode surface after immersion in strongly acidic solution. On the other hand, the MWCNT-chitosan films prepared from dispersions containing 1.0% chitosan loading, produced stable films even when left immersed for 24 h in strongly acidic solution. Thus, this concentration was chosen for further experiments.

2.4. Preparation of poly (brilliant green) modified electrodes

In order to study the effect of the DES acid doping agent on the formation rate and the electrochemical behaviour of poly(brilliant green) on carbon nanotubes, several acid doping solutions were tested with anions: sulfate (SO_4^{2-}), nitrate (NO_3^-), chlorate (Cl^-), carboxyl (COO^-).

PBG films were first formed by electropolymerization on MWCNT/GCE in an aqueous solution containing 1 mM BG + 0.5 M of different acids as doping agent, by potential cycling between −1.0 and 1.2 V vs. Ag/AgCl during 10 cycles at a scan rate of 50 mV s^{-1}. The electrochemical characteristics of each type of PBG film in the PBG/MWCNT/GCE configuration were investigated by cyclic voltammetry, and the best doping agent (sulfuric acid, see below) was chosen for electropolymerization in DES.

Ethaline DES, consisting of a 1:2 M ratio of choline chloride:ethylene glycol was prepared by prior heating of solid choline chloride to ~80 °C to evaporate any water, followed by addition of ethylene glycol under stirring and heating up to 100 °C until a homogeneous and colourless solution was obtained, which was cooled down to room temperature [24]. Since the monomer is not very soluble in strong acidic media, BG was first dissolved with a concentration just above 1.0 mM in a mixture containing 10% v/v of water: 90% v/v ethaline, which was thoroughly stirred and sonicated in an ultrasound bath in order to completely dissolve the monomer. This was followed by the addition of a tiny volume of the concentrated sulfuric acid doping agent, to finally obtain 1.0 mM BG monomer and 0.5 M of sulfuric acid, in the final mixture.

PBG_{DES} films on MWCNT/GCE were formed by using the same potential cycling parameters as in aqueous solution; the influence of the scan rate on the formation of the films was also investigated. For comparison purposes, PBG_{aq} on top of MWCNT was also prepared in an aqueous solution containing 1 mM BG in McIlvaine buffer, pH 4.0 during 10 cycles at a scan rate of 150 mV s^{-1}, as in Ref. [25]. The polymer films obtained were designated as $PBG_{ethaline}$50-200 and $PBG_{aq,}$ respectively.

2.5. Biosensor preparation

After optimization of the modified electrode architecture, GOx was immobilized on its surface by cross-linking, using a mixture of GOx with glutaraldehyde, as cross-linking agent, and BSA carrier protein. The enzyme solution was prepared by dissolving different amounts in the range 5.0–25 mg mL^{-1} of GOx in 0.1 M PB solution, pH 7.0. For all enzyme solutions, the same amount of BSA, 30 mg mL^{-1}, was added. For enzyme drop-coating, 1 μL of the enzyme solution containing BSA was dropped on a modified electrode surface followed by 1 μL of GA (2.5%). The electrode assembly was left to dry for 1 h at room temperature, after which the biosensor was immersed in buffer solution (pH 7.0) for at least 2 h before use in order to hydrate the formed membrane and facilitate the diffusion of ionic species. When not in use, the biosensor was kept in buffer solution at 4 °C to preserve enzyme activity.

3. Results and discussion

3.1. Polymerization in aqueous media - the influence of acid dopant on polymer growth

The polymerization of brilliant green was first carried out on MWCNT/GCE, by cycling the potential between −1.0 and 1.2 V vs. Ag/AgCl in 0.5 M aqueous solution of the acids H_2SO_4, HCl, HNO_3 and CH_3COOH at 50 mV s^{-1} (Supplementary Material Fig. S1). The supporting electrolyte plays an important role in the growth of conducting polymers. In the case of PBG, this has a big influence, since protonic acid doping of the polymer leads to a different mechanism of nucleation. This affects both the yield and the electrochemical behaviour of the formed films, as seen in the different voltammetric profiles (Supplementary Material Fig. S2).

The mechanism of polymerization of BG begins with oxidation of the secondary amino groups which form cation radicals and attack benzene rings in a free ortho-position relative to the amino group, initiating the polymerization. In different acid solutions, Fig. S1, similar behaviour was observed for all electropolymerizations, having one redox pair with midpoint potential value at ~0.5 V, with currents increasing in all cases, except for nitric acid solution, in which the peaks decrease with each cycle. In H_2SO_4, an oxidation peak at 0.8 V was also observed, which is attributed to monomer oxidation [21].

After electropolymerization for 10 cycles, the anodic peak currents at ~0.5 V were found to be 10.8, 4.94, 3.98, and 0.5 μA cm^{-2}, for PBG formed in solutions of the acids H_2SO_4, HCl, HCOOH and HNO_3, respectively. In the case of HNO_3, the polymer film was not stable as evidenced by the fact that the anodic peak current decreased with the number of cycles. Cyclic voltammograms recorded in 0.1 M PB pH 7.0 after polymerization, Fig. 1, also showed that the current peak corresponding to the polymer, ~0.5 V, was the highest for the film deposited in H_2SO_4. Taking into account the better-defined polymer peaks during polymerization, the presence of monomer oxidation peak, as well as higher polymer peak currents after polymerization, the conclusion was that H_2SO_4 would be the best choice of acid dopant for electropolymerization in DES.

3.2. Polymerization in ethaline - influence of scan rate

For BG electropolymerization in DES, a solution of 1.0 mM BG with 0.5 M H_2SO_4 in a 10% v/v of water: 90% v/v ethaline mixture was prepared, see experimental section for details. The PBG film was grown on MWCNT/GCE at scan rates in the range from 50 to 200 mV s^{-1}, during 10 cycles, sweeping the potential between −1.0 and 1.2 V vs. Ag/AgCl.

As seen in Fig. 1A–D, the amount of polymer formed increased with increasing scan rate, up to 150 mV s^{-1}; the decrease above this can be ascribed to diffusion limitations [26].

Cyclic voltammograms recorded in ethaline-H_2SO_4 (pH 2.0), Fig. 1A–D, for all sweep rates are quite similar, and the redox peaks are shifted towards more positive potentials compared with those of PBG$_{aq}$ electrodeposited in McIlvaine buffer (pH 4.0) aqueous solution, Fig. 1E. This shift is directly related to the pH, with protons being inserted from the solution into the polymer during the oxidation processes, and expelled during reduction. The oxidation peak currents recorded during the first five cycles increase continuously and indicate the formation of cation radicals. However, from the 5th to 10th cycles this increase slows down, due to the polymer deposited during the first cycles impeding further oxidation of the monomer on the electrode surface, so that hardly any radical cations and/or polymer are formed at this stage. Therefore, 10 cycles were selected for further electropolymerization studies. The same tendency is observed in the cyclic voltammograms for the polymerization of BG in aqueous solution, McIlvaine buffer (pH 4.0), at 150 mV s^{-1}, Fig. 1E.

3.3. Characterization of the nanostructured films

3.3.1. Cyclic voltammetry

To evaluate the electrochemical behaviour of PBG films electrodeposited on MWCNT/GCE, cyclic voltammograms of the modified electrodes were recorded in 0.1 M PB solution (pH 7.0) at a potential scan rate of 50 mV s^{-1}. Fig. 2 shows CVs of MWCNT/GCE modified with PBG$_{DES}$ electrodeposited at different scan rates, and PBG$_{aq}$ electrodeposited at 150 mV s^{-1}. As observed, the anodic and cathodic peak currents corresponding to the response of the PBG$_{DES}$ films increase with the electropolymerization scan rate, up to 150 mV s^{-1}. The decrease for PBG$_{DES}$ films electrodeposited at 200 mV s^{-1} may be attributed to the viscosity of the DES that makes diffusion of ionic species at higher sweep rate more difficult, as seen in Ref. [19]. PBG formed in aqueous medium, McIlvaine buffer (pH 4.0), exhibits lower peak currents than PBG$_{DES}$ films. The PBG$_{DES}$ film electrodeposited at 150 mV s^{-1} presented the highest currents and was therefore chosen as the best electrode platform for glucose oxidase immobilization.

3.3.2. Scanning electron microscopy

Fig. 3 displays SEM images of PBG films formed by electropolymerization on MWCNT modified carbon film electrodes in aqueous McIlvaine buffer solution (pH 4.0), and in ethaline DES at scan rates 50, 100, 150 and 200 mV s^{-1}. For comparison, an image of MWCNT on the carbon electrode support without electrodeposited polymer is also shown.

The SEM image in Fig. 3A shows a randomly entangled and cross-linked network of MWCNT spread over the electrode surface. The PBG formed by electropolymerization in aqueous McIlvaine buffer solution (pH 4.0), exists as a relatively thin film on the MWCNT surface, see Fig. 4B, which leads to only a slight increase in the diameter of the MWCNT.

The morphology of PBG$_{DES}$ films, that is those formed in ethaline, was examined as a function of the electropolymerization scan rate, Fig. 3C–F. The thickness of the polymer films is greater than that in aqueous McIlvaine buffer (pH 4.0). The PBG$_{DES}$ films from electropolymerization at 50 mV s^{-1}, Fig. 3C, exhibit a visibly rough and porous surface structure; at higher scan rates, there is formation of more compact and thicker nanostructures. For the PBG$_{DES}$ film made at 100 mV s^{-1}, a mix of compact and smooth areas with porous structures is observed, but for the films prepared at 150 and 200 mV s^{-1}, the formation of a more uniform and smooth surface is seen. This is in agreement with the literature [27,28] and can be explained based on the relative rates of
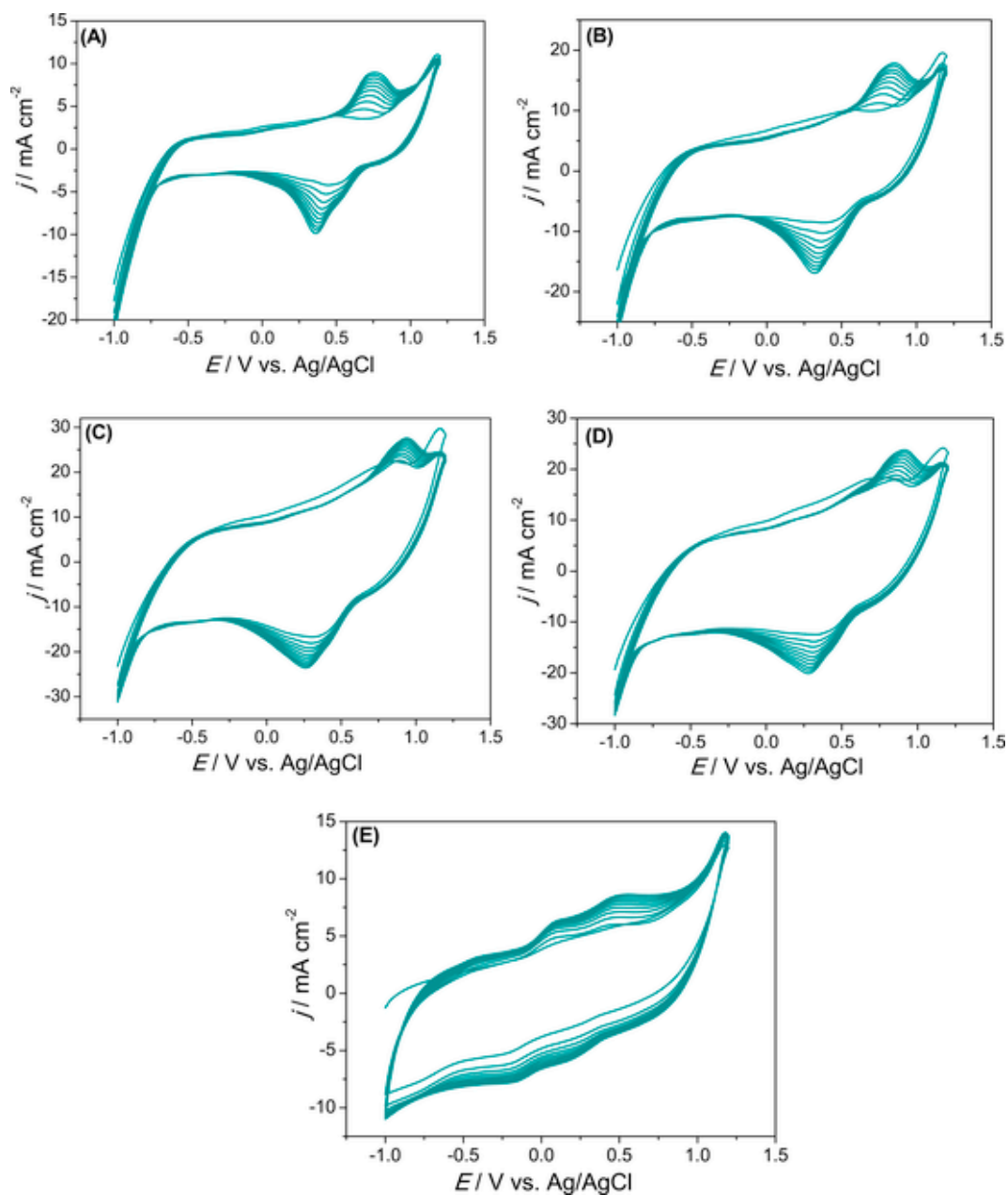
Fig. 1. CVs recorded during electropolymerization of BG on MWCNT/GCE in ethaline + (0.5 M H_2SO_4 + 10% H_2O) at scan rates: (A) $50\,mV\,s^{-1}$; (B) $100\,mV\,s^{-1}$; (C) $150\,mV\,s^{-1}$; (D) $200\,mV\,s^{-1}$; (E) electropolymerization of BG in aqueous McIlvaine buffer solution pH 4.0 at $150\,mV\,s^{-1}$.

nucleation and polymer growth. At slower scan rates, the number of nucleation sites generated on the MWCNT surface is smaller and the relatively large amount of time spent in the potential range of polymer oxidation leads to rapid growth of PBG nuclei. As a result, a thinner and rougher film is formed. On the other hand, at a higher scan rate, formation of more PBG nuclei is favoured, but less growth. As a result, Fig. 3C–F, a successively smoother and more compact surface is obtained, as the scan rate increases.

3.4. GOx/PBG$_{DES}$150/MWCNT/GCE biosensor for glucose determination

Enzyme biosensors for glucose determination using glucose oxidase immobilized on the best performing PBG modified MWCNT/GCE, with PBG deposited at $150\,mV\,s^{-1}$, were prepared according to the procedure described in the experimental section.

3.4.1. Influence of the applied potential

The influence of the applied potential on the GOx/PBG$_{DES}$150/MWCNT/GCE biosensor response towards $100\,\mu M$ glucose was performed in the range of -0.9 to $-0.2\,V$ vs. Ag/AgCl, Fig. 4. As can be seen, the response to glucose increments increases at less negative potential, between -0.9 and $-0.4\,V$, where the maximum was achieved, and then begins to decrease slightly. Therefore, an applied potential of $-0.4\,V$ vs. Ag/AgCl, was selected for further experiments.

3.4.2. Analytical performance

Fig. 5A displays the amperometric response for glucose at the GOx/PBG$_{DES}$150/MWCNT/GCE biosensor. Stock solutions of $1\,mM$ and $2\,mM$ glucose in $0.1\,M\,PB$ (pH 7.0) were prepared for glucose determination. The measurements were performed by the addition of aliquots
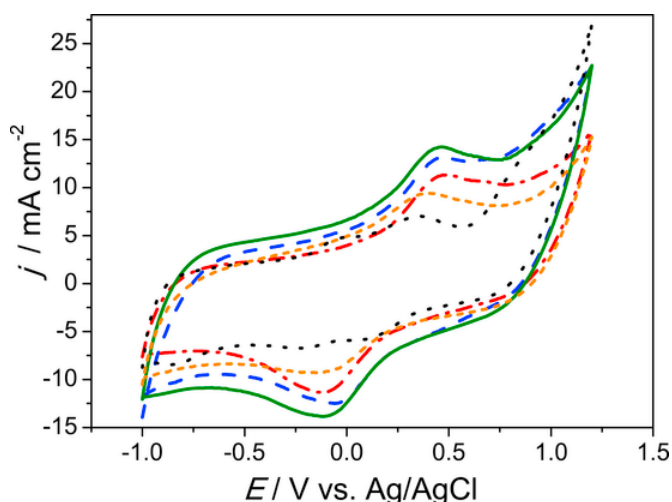
Fig. 2. CVs of PBG/MWCNT/GCE in 0.1 M PB solution (pH 7.0) at 50 mV s^{-1} (———): PBG$_{DES}$150-MWCNT/GCE (— — —); PBG$_{DES}$200-MWCNT/GCE (— · — · —); PBG$_{DES}$100-MWCNT/GCE (- - - - -); PBG$_{DES}$50-MWCNT/GCE; (· · · · ·) PBG$_{aqueous}$-MW-CNT/GCE.

of the stock glucose solutions to an electrochemical cell containing 0.1 M PB (pH 7.0) electrolyte solution, under continuous stirring at an applied potential of - 0.4 V vs. Ag/AgCl. A well-defined response rapidly reaching a stable plateau was recorded after each glucose addition, that was linear with glucose concentration in the range from 5 μM to 100 μM, Fig. 5B. The calibration curve followed the equation: Δj (μA cm^{-2}) = 1.33 + 0.54 [glucose] μM, and the limit of detection was estimated to be 2.33 μM, which is a better electrochemical performance than some of the most recent GOx biosensors for glucose determination in the literature [29–33], indicating advantages of preparing polymer films in deep eutectic solvent.

The binding affinity of the immobilized enzyme GOx with its substrate (glucose), the Hill constant, h, was estimated from the slope of the plot of log (I/I_{max}) versus log [glucose]. The Hill plot slope was 1.24; this value reflects positive cooperativity, h > 1 [34], meaning a high binding affinity of the immobilized enzyme (GOx) with its substrate and indicates that the reaction between enzyme and target analyte has Michaelis-Menten type kinetics. The Michaelis-Menten constant for GOx/PBG$_{DES}$150/MWCNT/GCE was estimated to be 53 μM.

3.5. GOx/PBG$_{DES}$150/MWCNT/GCE biosensor for inhibition measurements

3.5.1. Enzyme inhibition procedure

In order to evaluate the inhibition of the activity of glucose oxidase (GOx), amperometric measurements were made in 0.1 M PB solution (pH 7.0) at −0.4 V vs. Ag/AgCl. After stabilization of the baseline current, a chosen glucose concentration was added and the steady current recorded (I_0). Next, known concentrations of trace metal ions were added to inhibit the enzyme activity and the current was measured (I_1). The decrease in current is proportional to the concentration of inhibitor in solution. The percentage of inhibition, I %, is calculated according to Ref. [35]:

$$I\% = \frac{I_0 - I_1}{I_0} \times 100 \tag{1}$$

3.5.2. Optimization of the biosensor for inhibition

For optimizing the enzyme inhibition procedure, the effect of the loading of the immobilized enzyme and the pH value of the electrolyte were evaluated.

3.5.2.1. Influence of the enzyme loading The influence of the amount of immobilized enzyme was investigated at a constant concentration of BSA (30 mg mL^{-1}) and varying the concentration of GOx (5.0, 10.0, 15.0, 20.0, 25.0 and 30.0 mg mL^{-1}) immobilized on the optimised PBG$_{DES}$150/MWCNT/GCE electrode support, as described in the experimental section. The amperometric response to 0.5 mM glucose was tested for different enzyme loadings at an applied potential of - 0.4 V vs. Ag/AgCl. The total anodic change in current increases as the amount of GOx increases, reaching a maximum for 25.0 mg mL^{-1} GOx. For higher loadings, there is a decrease in biosensor response, indicating that high concentrations of enzyme compromise biosensor response due to diffusion limitations. The degree of inhibition for each enzyme loading was also assessed by evaluating the GOx activity in the presence of glucose by the addition of 20 nM of each metal ion in individual experiments. For all metals studied, the percentage of inhibition increased with increase in enzyme loading up to 20.0 mg mL^{-1} above which it remained the same. Therefore, 20.0 mg mL^{-1} of the enzyme was chosen as optimum.

3.5.2.2. Influence of the pH The enzyme biosensor response can depend significantly on the pH of the solution. The effect of the pH was investigated by comparing the sensitivities of the calibration curves obtained from additions of each inhibitor at GOx/PBG$_{DES}$150/MWCNT/GCE with 0.5 mM glucose as enzyme substrate, see Table 1. Amperometric measurements were performed at pH values between 6.0 and 8.0, at a fixed applied potential of −0.4 V vs. Ag/AgCl. The sensitivity to all trace metal ions increased from pH 6.0 to pH 7.0 and at pH 8.0 became lower again. This trend in the GOx response is the same as without the presence of inhibitors. Hence, pH 7.0 was selected as the more suitable pH value.

3.5.3. Inhibition measurements

3.5.3.1. Determination of the type of inhibition The mode of interaction between the metal ions and the active site of GOx, in the mechanism of reversible inhibition of Hg^2, Cd^{2+}, Pb^{2+} and, Cr^{VI} was deduced from plots of the percentage of inhibition versus inhibitor concentration, for various substrate concentrations. The traditional method requires both Dixon and Cornish-Bowden plots to fully elucidate the type of inhibition because Dixon plots for mixed and competitive inhibition are similar and from the Cornish-Bowden plot it is not possible to determine the inhibition constant for competitive inhibition [36,37]. In the new method [20], the effect of different substrate concentrations on I_{50} (concentration of inhibitor necessary to inhibit 50% of the initial response to the substrate) is evaluated. Here, following preliminary experiments with a wide range of glucose concentrations starting from low values, three concentrations: 0.25, 0.5 and 1.0 mM were employed, as shown in Fig. 6. For competitive inhibition, when the substrate concentration increases, the value of I_{50} also increases, and the maximum inhibition decreases, observed for Hg^{2+} and Cd^{2+}, Fig. 6A and B. On the other hand, when the values of I_{50} decrease with increasing substrate concentration, and the maximum inhibition value increases, the mechanism is uncompetitive inhibition, as seen for Pb^{2+}, Fig. 6C. Finally, for mixed inhibition, Fig. 6D, only a slight change in I_{50} occurs, as happens with Cr^{VI}. For comparison and verification purposes, the mechanism of inhibition was also evaluated from the corresponding Dixon and Cornish-Bowden plots and the same conclusions regarding the mechanism of reversible inhibition were reached for all four ions (see plots in Supplementary Material Fig. S3). The mechanism of inhibition for each metal ion agrees with that reported in the literature [13,39–41].

3.5.3.2. Analytical determination of Hg^2, Cd^{2+}, Pb^{2+} and Cr^{VI} ions As seen above, the concentration of the enzyme substrate needs to be carefully chosen. Fig. 6, that gives the response for 0.25, 0.5 and 1.0 mM glucose, shows that for 0.25 mM enzyme substrate, after the first addi-
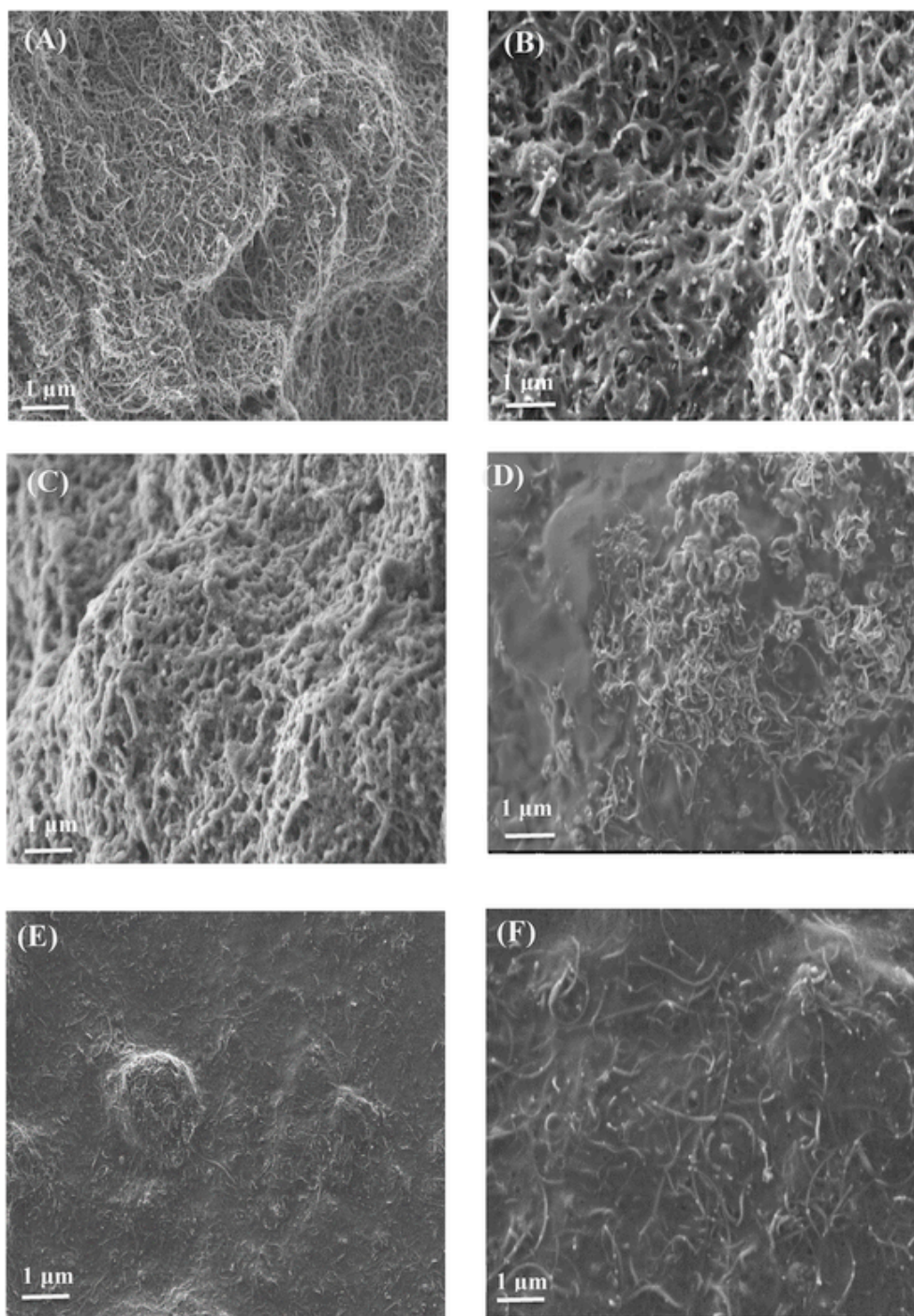
Fig. 3. SEM images on carbon film electrodes of (A) MWCNT; (B) PBG$_{aq}$/MWCNT (electropolymerized at 150 mV s^{-1}); (C) PBG$_{ethaline}$50/MWCNT; (D) PBG$_{ethaline}$100/MWCNT; (E) PBG$_{ethaline}$150/MWCNT; (F) PBG$_{ethaline}$200/MWCNT.

tion of inhibitor, more than 10% inhibition occurs. On the other hand, the maximum inhibition decreases with increase in glucose concentration, except for Pb^{2+}. Hence, the intermediate concentration of 0.5 mM glucose was chosen as the best value for inhibitor quantification.Under these conditions, the trace metal ions were determined at the GOx/PBG$_{DES}$150/MWCNT/GCE biosensor, and the limit of detection was calculated based on a signal-to-noise ratio of 3 (S/N = 3). From Fig. 6A, the linear range obtained for Hg^{2+} was 2.5–100 nM, with a LOD of 2.30 nM. For Cd^{2+}, Fig. 6B, the linear concentration range was 10–100 nM and the calculated LOD was 1.75 nM. Fig. 6C shows a linear response to Pb^{2+} from 10 to 120 nM presenting a LOD of 2.70 nM. Finally, for Cr^{VI}, Fig. 6D, the linear range was from 2.5 to 60 nM with the LOD of 2.44 nM.The enzyme inhibition constant (K_i) was estimated from the equations of the relationship between I_{50} and K_i, valid for all type of inhibition, as proposed by Amine et al. [20], Table 2. Hg^{2+}, Cd^{2+} and Cr^{VI} show the smallest values of K_i, which indicates a greater binding affinity, in agreement with the amount of these metal ions, expressed by I_{10}, necessary to inhibit enzyme activity, demonstrating
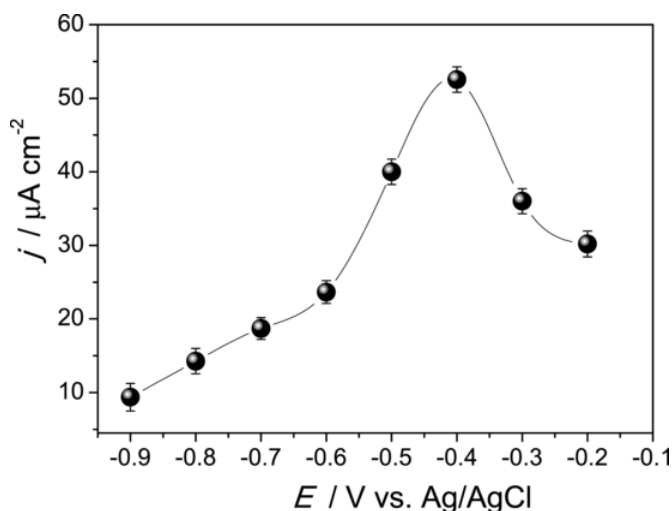
Fig. 4. Dependence of the glucose response at GOx/PBG$_{ethaline}$150/MWCNT/GCE on applied potential in 0.1 M PB solution (pH 7.0) in the presence of 100 μM glucose.
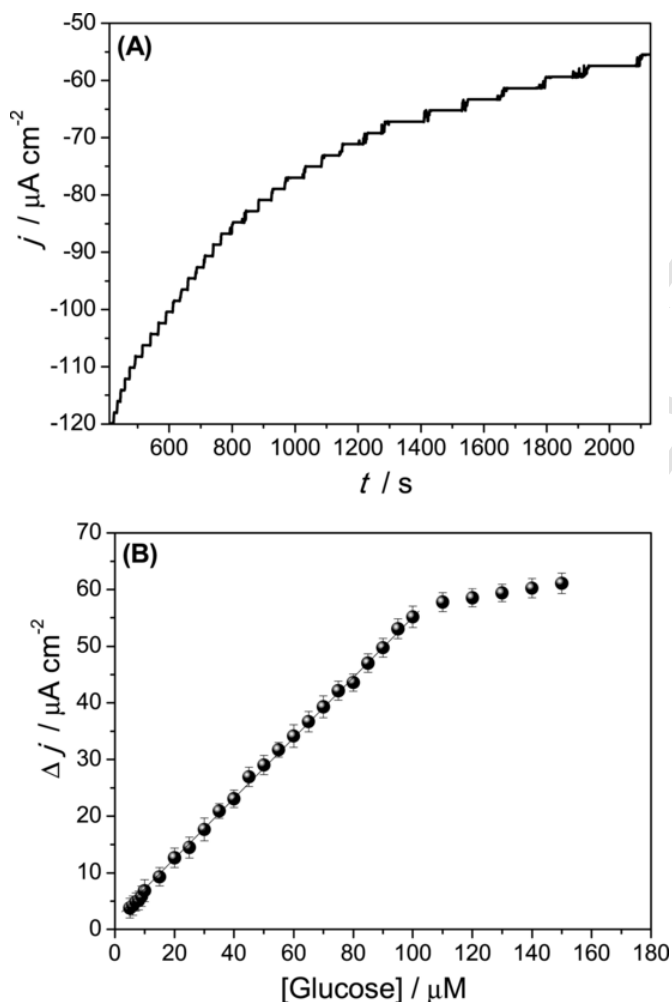

Fig. 5. (A) Amperometric response of GOx/PBG$_{ethaline}$150/MWCNT/GCE biosensor to glucose in 0.1 M PB solution, pH 7.0; applied potential −0.4 V vs. Ag/AgCl. (B) Calibration curve obtained from injection of increasing concentrations of glucose (0–150 μM).

their higher toxicity. On the other hand, Pb^{2+} presented a higher value of K_i, revealing its weaker inhibitor capability [38].The analytical performance of the novel GOx/PBG$_{DES}$/MWCNT/GCE biosensor for detec-

Table 1

Influence of the pH of the 0.1 M phosphate buffer supporting electrolyte solution on the sensitivity of determination of different metal ions, concentration 20 nM, at PBG$_{DES}$150/MWCNT/GCE biosensor by GOx inhibition in the presence of 0.5 mM glucose at applied potential −0.4 V vs. Ag/AgCl.

Metal ion	Sensitivity (μA cm^{-2} nM^{-1})			Inhibition (%)		
	pH 6.0	pH 7.0	pH 8.0	pH 6.0	pH 7.0	pH 8.0
Hg^{2+}	0.98	1.26	0.78	16.5	24.2	14.9
Cd^{2+}	0.90	1.16	0.84	17.0	22.2	11.3
Pb^{2+}	0.94	1.23	0.73	5.2	8.8	3.7
Cr^{VI}	0.86	1.15	0.78	11.2	23.2	7.2

tion of these toxic trace metal ions by the enzyme inhibition strategy was compared with the most relevant recent reports, Table 3. As can be seen, the novel biosensor showed superior electroanalytical performance to those found in the literature with the lowest limit of detection found until now. Furthermore, it does not require any kind of pre-treatment after each measurement for restoring GOx activity such as immersion of the electrodes in the buffer and/or metal chelating agent (EDTA) solution for a long period of time.The use of ethaline DES to form the PBG polymer film had a significant influence on its surface morphology, contributing to the improvement of the electroanalytical properties of PBG/MWCNT/GCE. The high sensitivity of the glucose biosensor and after immobilization of enzyme, can be attributed to a high binding affinity if the immobilized enzyme to the polymer film. This, in turn, increased the sensitivity in detection of trace metal ions by enzyme inhibition, for example compared with our previous studies on the same trace metal ions at redox polymer modified electrodes formed in aqueous solution, e.g. Ref. [42].

3.5.3.3. Selectivity Selectivity is a very important parameter in designing biosensors for application to real samples. Potential interferent ions were tested, the cations (Ag$^+$, K$^+$, Na$^+$, Fe^{3+}, Zn^{2+}, Ni^{2+}, Cu^{2+}, and Co^{2+}) and the anions (NO$_3^-$, SO$_4^{2-}$ and Cl$^-$), (Supplementary Material Fig. S4). Inhibition at the GOx/PBG$_{DES}$150/MWCNT/GCE biosensor was tested in the presence of 0.5 mM glucose at the previously optimised applied potential of −0.4 V vs. Ag/AgCl; the concentration of the interferents was 200 nM. This value corresponds to the maximum degree of inhibition achieved by all the trace biotoxic metal ions that are the object of this study. The degree of inhibition observed with the interferents had no significant influence of the initial response of glucose, less than 10%, for the high concentration of each interferent evaluated.

3.5.3.4. Repeatability and stability The repeatability of the GOx/PBG$_{DES}$/MWCNT/GCE biosensor was investigated by measuring the same concentration, 20 nM, of each trace metal ion at ten different modified electrodes prepared in the same way. The relative standard deviations were less than 4.5%.The stability of the biosensor was monitored daily by measuring the response of glucose, during 20 days, after successive inhibition experiments for all metal ions at the same modified electrode. When not in use, the biosensors were kept in buffer (PB, pH 7.0) at 4 °C. After 20 days, the glucose response lost just 13% of its initial value. However, such a loss of the enzyme activity does not compromise the use and the effectiveness of the inhibition biosensor.

3.5.3.5. Application In order to demonstrate the feasibility of the biosensor for food monitoring, the determination of trace metal ions in milk samples was carried out by the standard addition method. Milk samples were spiked with known amounts of Hg^{2+}, Cd^{2+}, Pb^{2+} and Cr^{VI} ions, and the recoveries were calculated, Table 4. The average apparent recovery was in the range of 99.5–100.1%, which indicates that the proposed biosensor is efficient for practical applications with an excellent level of reliability.
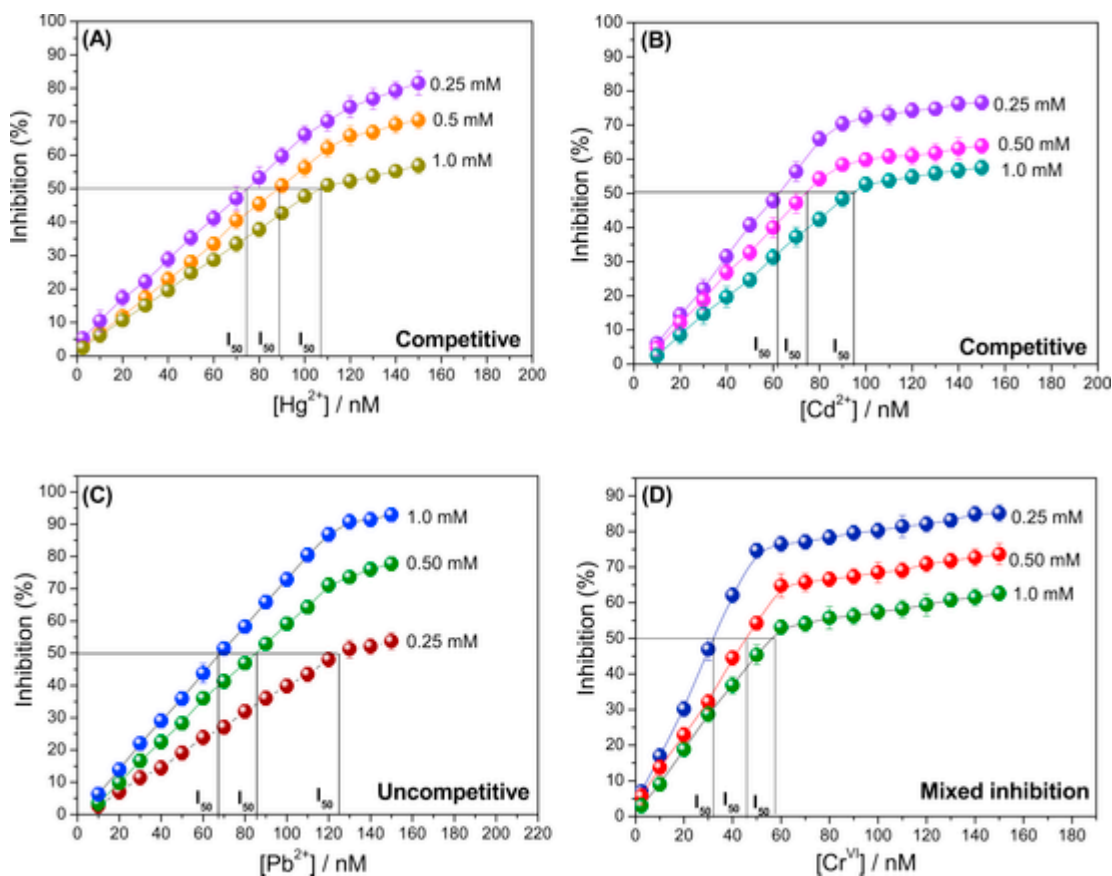
Fig. 6. Plots for determination of the mechanism of inhibition of the trace metal ions in 0.1 M PB solution (pH 7.0), according to Ref. [20], in the presence of three different concentrations of glucose at applied potential −0.4 V vs. Ag/AgCl.

Table 2
Parameters of inhibition obtained from the relationship between I_{50} and inhibition constant K_i. Equations from Ref. [20].

Metal ion	Mechanism of inhibition	Equation	K_i/nM	I_{10}/nM	I_{50}/nM
Hg^{2+}	Competitive	$\frac{I_{50}}{K_i} = \left(1 + \frac{[S]}{K_m}\right)$	8.39	15.4	88.0
Cd^{2+}	Competitive	$\frac{I_{50}}{K_i} = \left(1 + \frac{[S]}{K_m}\right)$	7.08	18.0	74.1
Pb^{2+}	Uncompetitive	$\frac{I_{50}}{K_i} = \left(1 + \frac{K_m}{[S]}\right)$	77.3	10.9	85.4
Cr^{VI}	Mixed	$\frac{I_{50}}{K_i} = 2\left(\frac{1 + \frac{[S]}{K_m}}{2 + \frac{[S]}{K_m}}\right)$	25.2	6.3	45.9

I_{10} - Concentration necessary for 10% inhibition of initial response of the substrate.
I_{50} - Concentration necessary for 50% inhibition of initial response of the substrate.
K_i - Inhibition constant.
K_m - Michaelis-Menten constant of the enzyme without the presence of inhibitor.
[S] – Enzyme substrate concentration.

4. Conclusions

A GOx inhibition biosensor for trace metal ion detection based on poly (brilliant green) – ethaline deep eutectic solvent/MWCNT has been developed for the first time. The deep eutectic solvent ethaline permitted the formation of polymer nanostructured films with superior sensing characteristics compared with films formed in aqueous solution, and thence the mediated glucose biosensor and enzyme inhibition biosensor. The mechanism of reversible inhibition was found to be competitive for Hg^{2+} and Cd^{2+}, uncompetitive for Pb^{2+} and mixed for Cr^{VI}. The novel enzyme inhibition biosensor exhibited a limit of detection of around 2 nM for all ions, with good selectivity and stability, sig-

nificantly lower than those in the literature. It was successfully applied to the detection of these trace metal ions in milk samples with excellent recoveries, which augurs well for its use in environmental trace metal ion monitoring.

Appendix A. Supplementary data

Supplementary data to this article can be found online at https://doi.org/10.1016/j.talanta.2019.120427.

Table 3

Comparison of performance of recent modified electrode-based enzyme biosensors using enzyme inhibition for trace metal ion determination.

Biosensor	Inhibitor	Mode of detection	Applied potential and pH	Linear range /μM	Detection limit/nM	Reactivation	Inhibition type	Ref.
PPy-GOx/Pt	Cd^{2+}	Amperometry	+0.7 V vs. (Ag/AgCl), pH 7.0	4.0–26	4000	EDTA, 2 mM (10 s)	competitive	[13]
	Pb^{2+}			1.6–7.7	1600		mixed	
	Hg^{2+}			0.48–3.3	480		non-competitive	
HRP/PNR/CFE	Cr^{VI}	Amperometry	- 0.5 V vs. (Ag/AgCl), pH 6.0	0.05–0.35	1600	–	uncompetitive	[39]
PPy-GOx/Pt	Cd^{2+}	Potentiometry	Zero current* vs.(Ag/AgCl), pH 7.0	0.04–62	44	phosphate buffer 0.05 M, (15 min)	competitive	[40]
	Pb^{2+}			0.10–15	24		non-competitive	
	Hg^{2+}			0.025–5.0	25		non-competitive	
GOx/PANI/Fc/Pt	Cr^{VI}	Amperometry	+0.7 V vs. (SCE), pH 2.55	0.49–95.73	9.0	phosphate buffer 0.05 M, (8 min)	*	[41]
PBG$_{DES}$150-MWCNT/GCE	Hg^{2+}	Amperometry	- 0.4 V vs. (Ag/AgCl), pH 7.0	0.0025–0.100	2.30	–	competitive	This work
	Cd^{2+}			0.010–0.080	1.75		competitive	
	Pb^{2+}			0.010–0.120	2.70		uncompetitive	
	Cr^{VI}			0.0025–0.060	2.44		mixed	

PPy-GOx/Pt – glucose oxidase (GOx) entrapped by polypyrrole (PPy) modified platinum electrode; HRP/PNR/CFE - horseradish peroxidase (HRP) immobilized on poly (neutral red) carbon film electrode; Urease/PVF/Pt - urease immobilized in poly(vinylferrocenium) film on Pt electrode; GOx/PANI/Fc/Pt - glucose oxidase (GOx) immobilized on polyaniline-ferrocene film on platinum electrode; GOx/PBG$_{DES}$-CNT/GCE - glucose oxidase (GOx) entrapped in poly (brilliant green) (PBG) electrodeposited on carbon nanotubes in the presence of the deep eutectic solvent ethaline; * not specified.

Table 4

Determination of trace metal ions in milk samples.

Metal ion	Added (nM)	Expected (nM)	Found (nM)	Apparent Recovery (%)
Hg^{2+}	20.0	20.0	19.9 ± 0.2	99.5
Cd^{2+}	20.0	20.0	20.2 ± 0.1	100.1
Pb^{2+}	20.0	20.0	19.8 ± 0.2	99.0
Cr^{VI}	20.0	20.0	19.8 ± 0.2	99.0

References

[1] M. Anastácio, A.P.M. dos Santos, M. Aschner, L. Mateus, Determination of trace metals in fruit juices in the Portuguese market, Toxicol. Rep. 5 (2018) 434–439, doi:10.1016/j.toxrep.2018.03.010.

[2] S. Millour, L. Noël, A. Kadar, R. Chekri, C. Vastel, V. Sirot, J.C. Leblanc, T. Guérin, Pb, C. Hg, As, Sb and Al levels in foodstuffs from the 2nd French total diet study, Food Chem. 126 (2011) 1787–1799, doi:10.1016/j.foodchem.2010.12.086.

[3] D. Tan, Y. He, X. Xing, Y. Zhao, H. Tang, D. Pang, Aptamer functionalized gold nanoparticles based fluorescent probe for the detection of mercury (II) ion in aqueous solution, Talanta 113 (2013) 26–30, doi:10.1016/j.talanta.2013.03.055.

[4] S. Ge, K. Wu, Y. Zhang, M. Yan, J. Yu, Paper-based biosensor relying on flower-like reduced graphene guided enzymatically deposition of polyaniline for Pb^{2+} detection, Biosens. Bioelectron. 80 (2016) 215–221, doi:10.1016/j.bios.2016.01.072.

[5] K.W. Huang, C.J. Yu, W.L. Tseng, Sensitivity enhancement in the colorimetric detection of lead(II) ion using gallic acid-capped gold nanoparticles: improving size distribution and minimizing interparticle repulsion, Biosens. Bioelectron. 25 (2010) 984–989, doi:10.1016/j.bios.2009.09.006.

[6] Z.S. Qian, X.Y. Shan, L.J. Chai, J.R. Chen, H. Feng, A fluorescent nanosensor based on graphene quantum dots-aptamer probe and graphene oxide platform for detection of lead (II) ion, Biosens. Bioelectron. 68 (2015) 225–231, doi:10.1016/j.bios.2014.12.057.

[7] Y. Ma, H. Liu, K. Qian, L. Yang, J. Liu, A displacement principle for mercury detection by optical waveguide and surface enhanced Raman spectroscopy, J. Colloid Interface Sci. 386 (2012) 451–455, doi:10.1016/j.jcis.2012.07.067.

[8] H. Bagheri, A. Afkhami, M. Saber-Tehrani, H. Khoshsafar, Preparation and characterization of magnetic nanocomposite of Schiff base/silica/magnetite as a preconcentration phase for the trace determination of heavy metal ions in water, food and biological samples using atomic absorption spectrometry, Talanta 97 (2012) 87–95, doi:10.1016/j.talanta.2012.03.066.

[9] J.L. Guzmán-Mar, L. Hinojosa-Reyes, A.M. Serra, A. Hernández-Ramírez, V. Cerdà, Applicability of multisyringe chromatography coupled to cold-vapor atomic fluorescence spectrometry for mercury speciation analysis, Anal. Chim. Acta 708 (2011) 11–18, doi:10.1016/j.aca.2011.09.037.

[10] W. Zeng, Y. Chen, H. Cui, F. Wu, Y. Zhu, J.S. Fritz, Single-column method of ion chromatography for the determination of common cations and some transition metals, J. Chromatogr., A 1118 (2006) 68–72, doi:10.1016/j.chroma.2006.01.065.

[11] L. Zhao, S. Zhong, K. Fang, Z. Qian, J. Chen, Determination of cadmium(II), cobalt(II), nickel(II), lead(II), zinc(II), and copper(II) in water samples using

dual-cloud point extraction and inductively coupled plasma emission spectrometry, J. Hazard Mater. 239–240 (2012) 206–212, doi:10.1016/j.jhazmat.2012.08.066.

[12] M.S. Thakur, K.V. Ragavan, Biosensors in food processing, J. Food Sci. Technol. 50 (2013) 625–641, doi:10.1007/s13197-012-0783-z.

[13] J.G. Ayenimo, S.B. Adeloju, Rapid amperometric detection of trace metals by inhibition of an ultrathin polypyrrole-based glucose biosensor, Talanta 148 (2016) 502–510, doi:10.1016/j.talanta.2015.11.024.

[14] L.I.N. Tomé, V. Baião, W. da Silva, C.M.A. Brett, Deep eutectic solvents for the production and application of new materials, Appl. Mater. Today 10 (2018) 30–50, doi:10.1016/j.apmt.2017.11.005.

[15] K.P. Prathish, R.C. Carvalho, C.M.A. Brett, Electrochimical characterisation of poly(3,4-ethylenedioxythiophene) film modified glassy carbon electrodes prepared in deep eutectic solvents for simultaneous sensing of biomarkers, Electrochem. Acta 187 (2016) 704–713, doi:10.1016/j.electacta.2015.11.092.

[16] K.P. Prathish, R.C. Carvalho, C.M.A. Brett, Highly sensitive poly(3,4-ethylenedioxythiophene) modified electrodes by electropolymerisation in deep eutectic solvents, Electrochem. Commun. 44 (2014) 8–11, doi:10.1016/j.elecom.2014.03.026.

[17] P.M.V. Fernandes, J.M. Campina, C.M. Pereira, F. Silva, Electrosynthesis of polyaniline from choline-based deep eutectic solvents: morphology, stability and electrochromism, J. Electrochem. Soc. 159 (2012) 97–105, doi:10.1149/2.059209jes.

[18] F. Wang, F. Zou, X. Yu, Z. Feng, N. Du, Y. Zhong, X. Huang, Electrochemical synthesis of poly (3-aminophenylboronic acid) in ethylene glycol without exogenous protons, Phys. Chem. Chem. Phys. 18 (2016) 9999–10004, doi:10.1039/C6CP00800C.

[19] O. Hosu, M.M. Bârsan, C. Cristea, R. Săndulescu, C.M.A. Brett, Nanostructured electropolymerized poly(methylene blue) films from deep eutectic solvents. Optimization and characterization, Electrochim. Acta 232 (2017) 285–295, doi:10.1016/j.electacta.2017.02.142.

[20] A. Amine, L. El Harrad, F. Arduini, D. Moscone, G. Palleschi, Analytical aspects of enzyme reversible inhibition, Talanta 118 (2014) 368–374, doi:10.1016/j.talanta.2013.10.025.

[21] M.E. Ghica, R. Pauliukaite, O. Fatibello-Filho, C.M.A. Brett, Application of functionalised carbon nanotubes immobilised into chitosan films in amperometric enzyme biosensors, Sens. Actuators B Chem. 142 (2009) 308–315, doi:10.1016/j.snb.2009.08.012.

[22] P. Papakonstantinou, R. Kern, L. Robinson, H. Murphy, J. Irvine, E. McAdams, J. McLaughlin, T. McNally, Fundamental electrochemical properties of carbon nanotube electrodes, Fullerenes Nanotub. Carbon Nanostructures 13 (2005) 91–108, doi:10.1081/FST-200050684.

[23] N.S. Lawrence, R.P. Deo, J. Wang, Comparison of the electrochemical reactivity of electrodes modified with carbon nanotubes from different sources, Electroanalysis 17 (2005) 65–72, doi:10.1002/elan.200403120.

[24] A.P. Abbott, D. Boothby, G. Capper, D.L. Davies, R.K. Rasheed, Deep Eutectic Solvents formed between choline chloride and carboxylic acids: versatile alternatives to ionic liquids, J. Am. Chem. Soc. 126 (2004) 9142–9147, doi:10.1021/ja048266j.

[25] M.E. Ghica, C.M.A. Brett, Poly(brilliant green) and poly(thionine) modified carbon nanotube coated carbon film electrodes for glucose and uric acid biosensors, Talanta 130 (2014) 198–206, doi:10.1016/j.talanta.2014.06.068.

[26] W.A. Badawy, K.M. Ismail, S.S. Medany, Optimization of the electropolymerization of 1-amino-9,10-anthraquinone conducting films from aqueous media, Electrochim. Acta 51 (2006) 6353–6360, doi:10.1016/j.electacta.2006.04.021.

[27] S. Mu, Y. Yang, Spectral characteristics of polyaniline nanostructures synthesized by using cyclic voltammetry at different scan rates, J. Phys. Chem. B 112 (2008) 11558–11563, doi:10.1021/jp8051517.

[28] A. Kellenberger, D. Ambros, N. Plesu, Scan rate dependent morphology of polyaniline films electrochemically deposited on nickel, Int. J. Electrochem. Sci. 9 (2014) 6821–6833. http://www.electrochemsci.org.

[29] R. Devasenathipathy, V. Mani, S.M. Chen, S.T. Huang, T.T. Huang, C.M. Lin, K.Y. Hwa, T.Y. Chen, B.J. Chen, Glucose biosensor based on glucose oxidase immobilized at gold nanoparticles decorated graphene-carbon nanotubes, Enzym. Microb. Technol. 78 (2015) 40–45, doi:10.1016/j.enzmictec.2015.06.006.

[30] A.P. Periasamy, Y.J. Chang, S.M. Chen, Amperometric glucose sensor based on glucose oxidase immobilized on gelatin-multiwalled carbon nanotube modified glassy carbon electrode, Bioelectrochemistry 80 (2011) 114–120, doi:10.1016/j.bioelechem.2010.06.009.

[31] S. Palanisamy, C. Karuppiah, S.M. Chen, Direct electrochemistry and electrocatalysis of glucose oxidase immobilized on reduced graphene oxide and silver nanoparticles nanocomposite modified electrode, Colloids Surfaces B Biointerfaces 114 (2014) 164–169, doi:10.1016/j.colsurfb.2013.10.006.

[32] F.Y. Kong, S.X. Gu, W.W. Li, T.T. Chen, Q. Xu, W. Wang, A paper disk equipped with graphene/polyaniline/Au nanoparticles/glucose oxidase biocomposite modified screen-printed electrode: toward whole blood glucose determination, Biosens. Bioelectron. 56 (2014) 77–82, doi:10.1016/j.bios.2013.12.067.

[33] T. Homma, D. Sumita, M. Kondo, T. Kuwahara, M. Shimomura, Amperometric glucose sensing with polyaniline/poly(acrylic acid) composite film bearing covalently-immobilized glucose oxidase: a novel method combining enzymatic glucose oxidation and cathodic O_2 reduction, J. Electroanal. Chem. 712 (2014) 119–123, doi:10.1016/j.jelechem.2013.11.009.

[34] J.M. Berg, J.L. Tymoczko, L. Stryer, Biochemistry, fifth ed., 2006, p. 1120, doi:10.1007/s13398-014-0173-7.2.

[35] B. Elsebai, M.E. Ghica, M.N. Abbas, C.M.A. Brett, Catalase based hydrogen peroxide biosensor for mercury determination by inhibition measurements, J. Hazard Mater. 340 (2017) 344–350, doi:10.1016/j.jhazmat.2017.07.021.

[36] M. Dixon, The determination of enzyme inhibitor constants, Biochem. J. 55 (1953) 170–171, doi:10.1042/bj0550170.

[37] A. Cornish-Bowden, A simple graphical method for determining the inhibition constants of mixed, uncompetitive and non-competitive inhibitors (*Short Communication*), Biochem. J. 137 (1974) 143–144, doi:10.1042/bj1370143.

[38] K. Ramírez-Sánchez, F. Alvarado-Hidalgo, I. Ardao, R. Starbird-Pérez, Enzymatic inhibition constant of acetylcholinesterase for the electrochemical detection and sensing of chlorpyrifos, J. Nat. Resour. Dev. 8 (2018) 9–14, doi:10.5027/jnrd.v8i0.02.

[39] A. Attar, M.E. Ghica, A. Amine, C.M.A. Brett, Poly(neutral red) based hydrogen peroxide biosensor for chromium determination by inhibition measurements, J. Hazard Mater. 279 (2014) 348–355, doi:10.1016/j.jhazmat.2014.07.019.

[40] J.G. Ayenimo, S.B. Adeloju, Inhibitive potentiometric detection of trace metals with ultrathin polypyrrole glucose oxidase biosensor, Talanta 137 (2015) 62–70, doi:10.1016/j.talanta.2015.01.006.

[41] G.M. Zeng, L. Tang, G.L. Shen, G.H. Huang, C.G. Niu, Determination of trace chromium (VI) by an inhibition-based enzyme biosensor incorporating an electropolymerized aniline membrane and ferrocene as electron transfer mediator, Int. J. Environ. Anal. Chem. 84 (2004) 761–774, doi:10.1080/03067310410001730619.

[42] M.E. Ghica, C.M.A. Brett, Glucose oxidase inhibition in poly(neutral red) mediated enzyme biosensors for heavy metal determination, Microchim. Acta 163 (2008) 185–193, doi:10.1007/s00604-008-0018-1.